

## Blast load induced response and the associated damage of buildings considering SSI

Sayed Mahmoud\*

*Department of Construction Engineering, College of Engineering, Dammam University, Saudi Arabia*

*(Received February, 2014, Revised March 17, 2014, Accepted April 13, 2014)*

**Abstract.** The dynamic response of structures under extremely short duration dynamic loads is of great concern nowadays. This paper investigates structures' response as well as the associated structural damage to explosive loads considering and ignoring the supporting soil flexibility effect. In the analysis, buildings are modeled by two alternate approaches namely, (1) building with fixed supports, (2) building with supports accounting for soil-flexibility. A lumped parameter model with spring-dashpot elements is incorporated at the base of the building model to simulate the horizontal and rotational movements of supporting soil. The soil flexibility for various shear wave velocities has been considered in the investigation. In addition, the influence of variation of lateral natural periods of building models on the obtained response and peak response time-histories besides damage indices has also been investigated under blast loads with different peak over static pressures. The Dynamic response is obtained by solving the governing equations of motion of the considered building model using a developed Matlab code based on the finite element toolbox CALFEM. The predicted results expressed in time-domain by the building model incorporating SSI effect are compared with the corresponding model results ignoring soil flexibility effect. The results show that the effect of surrounding soil medium leads to significant changes in the obtained dynamic response of the considered systems and hence cannot be simply ignored in damage assessment and response time-histories of structures where it increases response and amplifies damage of structures subjected to blast loads. Moreover, the numerical results provide an understanding of level of damage of structure through the computed damage indices.

**Keywords:** blast loads, soil-structure interaction, dynamic response, damage index

### 1. Introduction

Bomb detonations, due to spread of terrorist attacks, on public buildings have become hazardous and led to severe damages and loss of lives all over the world (Osteraas 2006). The design and construction of important buildings to provide life safety against explosions became an important issue from structural engineer's point of view (Elliot *et al.* 1992). After the occurrence of a blast, high-pressure shock waves are formed and expand outward from the center of explosion (Baker *et al.* 1983, Forbes 1999, Smith and Hetherington 1994). The strength of the blast pressure exerted on the surface of the building may be of intensity greater than the force for which the

---

\*Corresponding author, Assistant Professor, E-mail: [elseedy@hotmail.com](mailto:elseedy@hotmail.com)

<sup>a</sup>Assistant Professor, E-mail: [elseedy@hotmail.com](mailto:elseedy@hotmail.com)

building is designed. In order to understand a structure's resistance to explosives, its structural response must be evaluated. To predict the realistic response of structures under blast loads, an accurate prediction of the pressure-time history at various points on the structure is required where the induced pressure from shock waves decay with distance measured from the explosion source as well as time. Structural behavior under explosive loads is a major concern in structural engineering and understanding of the response and damage is important to provide guidance in post disaster evacuations and post blast rehabilitations. Over the last few decades, significant research efforts have been conducted in trying to recognize the effect of an explosion on the structure and its elements (Houlston and DesRochers 1987, Rudrapatana *et al.* 1999, Jacinto *et al.* 2001). Recently, a lot of relevant research concerning the blast induced structural response has been expended numerically. The structural elements such as the beams, columns and plates (Shi *et al.* 2007), and the whole structure (Luccioni 2004), have been simulated and studied. In order to evaluate the structural damage and mitigate the associated risk, the response of structures under short duration loads, blast and impact loadings, have been extensively studied (Boutros 2000, Krauthammer *et al.* 1990, Schleyer and Hsu 2000). Analysis and assessment of damage of modeled cable-stayed bridges subjected to explosive loads can be found in (Edmond *et al.* 2010, Hong *et al.* 2010).

A review of the above cited papers indicates that the analyses ignore the influence of SSI on the dynamic response of structures as well as the induced damage.

The influence of the interaction of the soil with a superstructure on its dynamic behavior has been the subject of some investigations. Kumart M. *et al.* (2010) studied the response of semi-buried structure subjected to non-contact blast loading comparing the peak stresses and displacements by varying the scaled distance of the explosion, the buried depth of the structure and the type of soil. Liu H. (2009) used the ABAQUS finite-element software package to model the influence of critical parameters such as soil compressibility and blast impulses on the dynamic soil-structure interaction. Moreover, Huang, X. *et al.* (2011) adopted a generalized iteration procedure to analyze the non-constancy of soil flexibility and the pulse shape effect on the damage of buried RC structure under blast load. In addition, Jayasinghe L.B. *et al.* (2013) employed an explicit nonlinear finite element analysis technique to examine the response of a pile foundation in saturated sand considering complex material behavior of soil and soil-pile interaction. Damage assessment of buried structures against both internal and external blast loads incorporating SSI effect has also been addressed (Ma *et al.* 2008, 2010).

Although the above cited papers consider SSI effects on the expected structural response and the associated damage, it has been found that most of them have been focused on the response of buried and semi-buried structures, which exhibit quite different dynamic characteristics comparing to constructed above ground buildings.

This research aims to provide a better understanding of the dynamic response behavior and damage of buildings under blast loads due to incorporation of the base soil flexibility. The present study provides a comparative approach in which the responses of both rigid or fixed base building model and flexible base building model are studied extensively. Numerical simulations are performed under different impact load intensities and various influential parameters. In the numerical simulation, several shear wave velocities of the supporting soil are introduced to evaluate the response and potential damage to the superstructure due to explosions. Moreover, the effect of change in the lateral natural periods on the building's response and damage due to inclusion of the of soil-flexibility effect has also been presented to gain some insight into the

behavior buildings rested on flexible base soil and exposed to explosions. Such a study may help in providing guidelines to assess in a more accurate way the explosions vulnerability of the buildings and may be useful for blast-resistant design.

## 2. Load discription

The explosion of ideal form can be divided into two parts. The first part is called the positive phase in which the pressure is over the ambient atmospheric pressure. In the second part which is called negative phase or under pressure phase, the pressure drops to below the ambient atmospheric pressure causing suction, see Fig. 1. Explosion in the air involves extremely sudden and rapid release of energy. This energy rapidly propagates in the form of high temperature, light, sound and shock waves. This shock blast air waves represent the major part of the released energy. From a structural point of view, these waves are considered as the more significant in the study of damage in buildings due to the explosive event where the blast waves propagate through the air and encircle the structure and all its surfaces so that the whole structure is exposed to the blast pressure. The charge weight and the stand-off distances are considered as two important parameters to describe the threat of a conventional explosion.

Hopkinson's approach for blast wave scaling is considered as the most widely used one. In the approach, an explosive charge  $W$ , expressed in Kilograms of TNT, at any distance  $R$  can be transformed into a characteristic scaled distance  $Z$  as (Baker *et al.* 1983):

$$Z = \frac{R}{W^{1/3}} \quad (1)$$

Blast loads in simple geometries can be predicted empirically or semi-empirically. The pressure as a function of time  $t$  in an assumed exponential form can be expressed mathematically according to Kinny and Graham (1985) as:

$$P(t) = P_{so} \left(1 - \frac{t}{t_o}\right) e^{\left(-\frac{bt}{t_o}\right)} \quad (2)$$

Where  $P_{so}$  is the peak overpressure,  $t_o$  is the duration of the positive phase of the blast load,  $b$  is the wave form or decay parameter and  $P(t)$  is the pressure at time  $t$ .

In Eq. (2), the overpressure  $P_{so}$  in Pascal is calculated by (Kinny and Graham 1985) as:

$$P_{so} = \frac{808 P_a \left[1 + \left(\frac{Z}{4.5}\right)^2\right]}{\sqrt{1 + \left(\frac{Z}{0.048}\right)^2} \sqrt{1 + \left(\frac{Z}{0.32}\right)^2} \sqrt{1 + \left(\frac{Z}{1.35}\right)^2}} \quad (3)$$

in which  $P_a$  is the atmospheric pressure. The positive loading duration in milliseconds is expressed as follows (Kinny and Graham 1985):

$$t_o = \frac{908 W^{1/3} \left[1 + \left(\frac{Z}{0.54}\right)^{10}\right]}{\left[1 + \left(\frac{Z}{0.02}\right)^3\right] \left[1 + \left(\frac{Z}{0.74}\right)^6\right] \sqrt{1 + \left(\frac{Z}{6.9}\right)^2}} \quad (4)$$

The decay factor  $b$  is available in (Kinny and Graham 1985) with tabulated data varying with scaled distance  $Z$

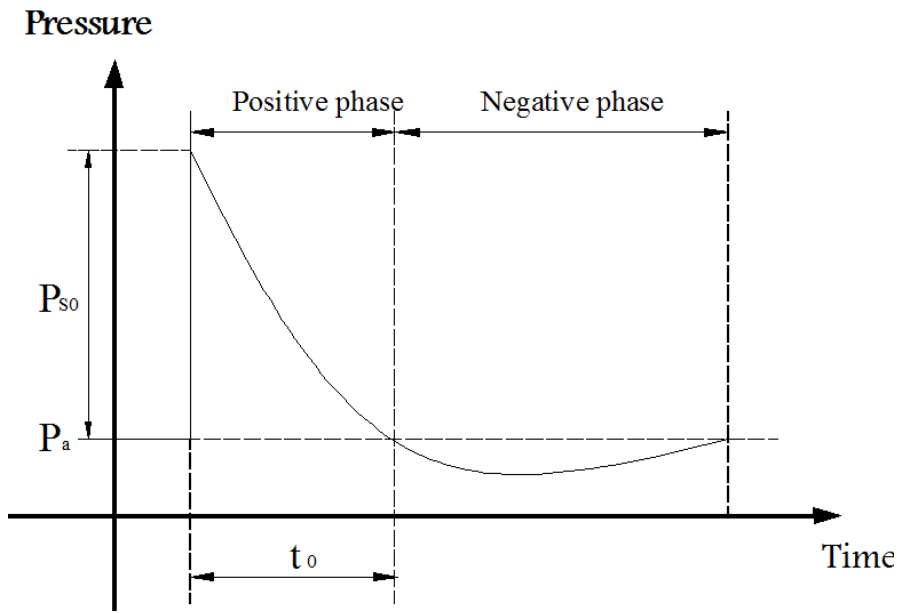


Fig. 1 Typical pressure time-history for an explosion

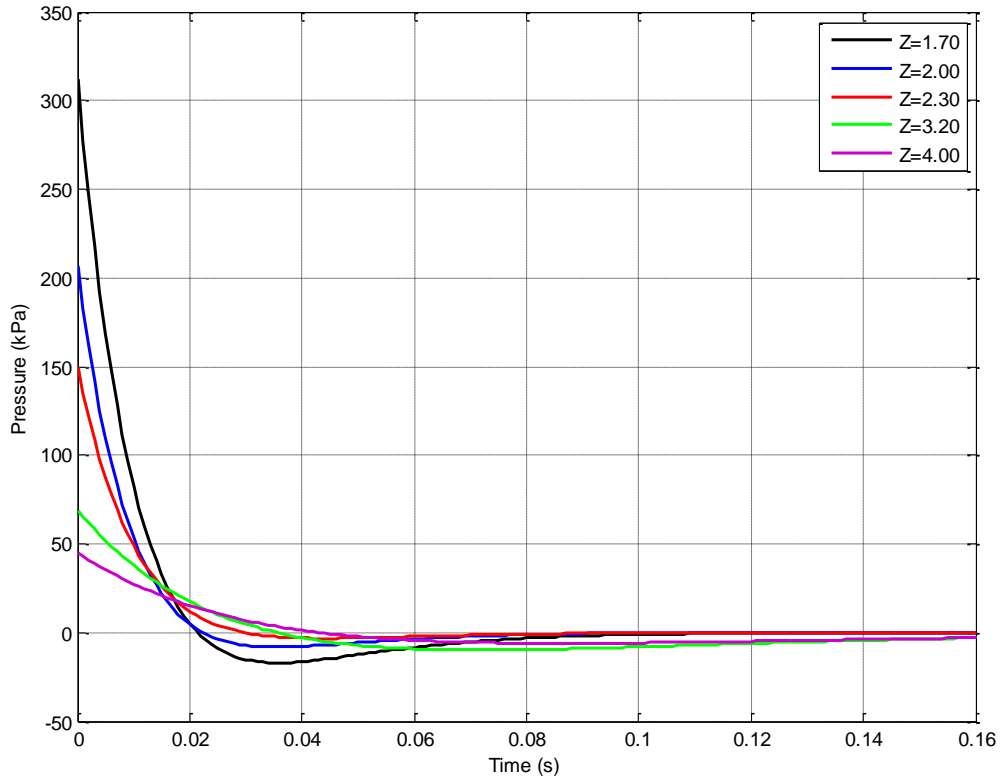


Fig. 2 Pressure time-histories for different explosions

Typical reflected pressure time-histories can be seen in Fig. 2 which involved a TNT charge weight of 10 Kg located at different stand-off distances ranging from 3.5 to 8 m. Rapidly rising peak pressures can be seen from the figure and followed by a decay towards the ambient pressure within the positive phase duration. With further decrease, the pressure time-histories drop to below the ambient atmospheric pressure causing suction, i.e., negative pressure phase.

### 3. Damage Indices

In the design criteria, study against collapse is considered as the main objective. However, performance in terms of functionality and economy is still the central role. Great efforts are made to improve the methods of resistant design against dynamic loads such as earthquake, wind and blast loadings not only to avoid failure under these destructive loads but also to limit damage under moderate loads. The use of damage indices and damage measures for structures under dynamic loads are widely used. They aim to clarify the different approach methodologies (Kappos 1997, Powell and Allahabadi 1988, Cosenza *et al.* 1993) and to detail different proposed formulations (McCabe and Hall 1989, Williams and Sexsmith 1995, Fardis 1995).

One of the key parameters used to identify structural damage is the kinematic and cyclic ductility which can be defined as a function of rotation, curvature or displacement. The amount of kinematic energy dissipated during loadings is another key for structural damage. To date most available damage models either only use ductility as a damage measure neglecting the amount of dissipated energy effect or define the structural damage as a function of the maximum ductility and the energy dissipated under the applied loads. Powell and Allahabad (1988) proposed a damage index in terms of the maximum plastic displacement independent of the amount of dissipated energy. The formula used to define the damage index in terms of maximum displacement  $U_{max}$ , yield displacements  $U_y$  and the ultimate displacement  $U_u$  can be written as (Powell and Allahabad 1988)

$$DI_{AP} = \frac{U_{max} - U_y}{U_u - U_y} \quad (5)$$

Damage indices based on the kinematic or cyclic ductility as a measure for damage assume that structural model collapse is mainly due to the induced maximum plastic displacement, and neglect the effect of both the number of plastic cycles and the energy dissipated under the applied dynamic load. However, it has been shown these indices can be used for structures with cumulative deterioration such as in the case of impulse-type or short-duration earthquakes which are characterized by one cycle with a large plastic displacement and others with a small amount of plastic work.

A damage index based on the structure hysteretic energy has been proposed by Fajfar (1992) and Cosenza *et al.* (1993)

$$DI_{FC} = \frac{E_H / (F_y U_y)}{\mu_u - 1} \quad (6)$$

In which  $E_H$ ,  $F_y$  and  $\mu_u$  are the hysteretic dissipation energy, yield strength and ultimate ductility respectively.

The Park-Ang damage index which defines the structural damage in terms of both the maximum dynamic response, i.e., maximum plastic displacement, and hysteretic energy dissipated,

can be expressed as follows (Park and Ang 1985, Park *et al.* 1985, 1987):

$$DI_{PA} = \frac{U_{max}}{U_u} + \frac{\beta}{F_y U_u} \int dE \quad (7)$$

where  $dE$  is the incremental absorbed hysteretic energy and  $\beta$  is a nonnegative parameter. The level of damage can be defined based on the values of captured damage indices in which the building can be considered as having insignificant damage for assigned damage index  $DI < 0.2$ . While for  $DI < 0.5$  damage can be considered as repairable. For  $0.5 < DI < 1$  the structure did not collapse but it could not be considered as repairable. However, for  $DI \geq 1.0$  total damaged of the structure occur (Park *et al.* 1987). All the aforementioned damage indices will be used in the section devoted to the parametric study.

#### 4. Methods of structural analysis

This section introduces the mathematical formulation for the building and the soil base by which the response of a structure to specified loads and actions is determined. This response is measured by determining the internal forces or stress, energies and displacements or deformations throughout the structure.

##### 4.1 Structural building model

The schematic representation of the idealized SDOF mathematical model for a building of height  $h_1$  is shown in Fig. 3. The use of SDOF system for predicting dynamic response of structure exposed to blast load is considered as simple and cost-effective approach that requires less computational effort. As can be seen, Fig. 3 presents a rigid deck of mass  $m_1$  connected to a rigid mat of mass  $m_b$  through massless columns of stiffness  $k_1$  and damping coefficient  $c_1$ . The values of structural stiffness and damping coefficients can be calculated from the formulas in (Harris 2002). The dynamic equations of motion expressed in matrix form considering and ignoring SSI can be written based on the lumped mass model in Fig. 3 and will be presented in Section 5.

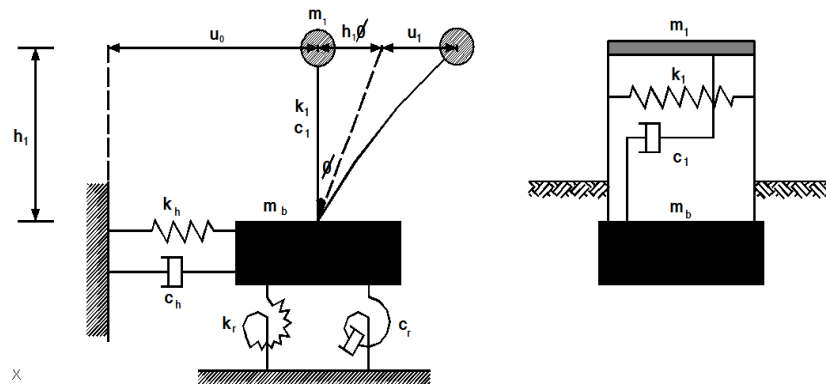


Fig. 3 Idealized SDOF building model

#### 4.2 Base soil model

The discrete model has been formulated for the mat foundations embedded in the halfspace and located at the base of the structure to represent the soil and interaction mechanisms (Whitman 1967). Springs and dashpots have been employed in the model in order to account for the transitional and rotational movements of the soil including damping. For a raft of length  $L$  and width  $B$ , the parameters of springs and dashpots for sway and rocking, which represent the SSI, are computed using the following expressions (Whitman 1967):

$$k_h = 2(1-\nu)G\beta_x\sqrt{BL}, c_h = 0.576k_h r_h \sqrt{\frac{\rho}{G}}$$

$$k_r = \frac{G}{1-\nu}\beta_\phi BL^2, c_r = \frac{0.3}{1+\beta_\phi}k_r r_r \sqrt{\frac{\rho}{G}} \quad (8)$$

where  $\nu$  is the Poisson's ratio of the soil,  $G$  is the shear modulus,  $\beta_x$  and  $\beta_\phi$  are the correct constants of swaying and rocking springs, respectively;  $\rho$  is the density of soil.  $r_h$  and  $r_r$  denotes the equivalent radii of foundation base for swaying and rocking spring-dampers, respectively. The maximum shear modulus at low strain  $G_{\max}$  is related to the shear wave velocity  $V_s$  according to the following expression (Whitman 1967):

$$G_{\max} = \rho(V_s)^2 \quad (9)$$

The shear modulus used in the analysis incorporating the SSI has been reduced in order to maintain closer behaviour of the soil. The modulus reduction curves  $(G/G_{\max} - \gamma)$  are often used to solve dynamic problems when shear strains  $\gamma$  drive the soil beyond its elastic range. As the soil enters into the inelastic stage, the shear modulus of the soil is reduced substantially what is correspondingly related to the decrease in the shear wave velocity. In the case of the study conducted, the reduced shear modulus  $G$  has been assumed to be 50% of  $G_{\max}$  calculated according to Eq. (9) (see (Whitman 1967)):

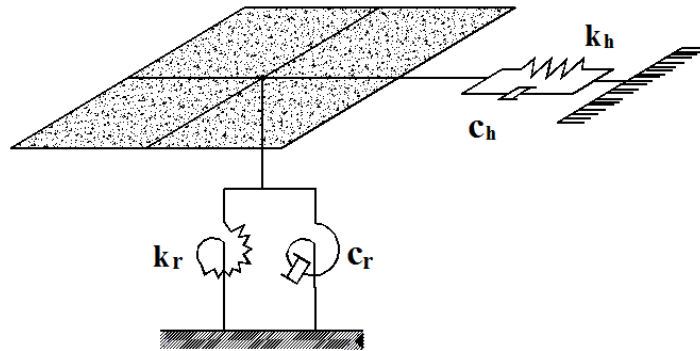


Fig. 4 Equivalent soil springs and dashpots to model horizontal and rotational soil movements

## 5. Governing equation of motion

The governing equation of motion for the building system shown in Fig. 3 due to impact load  $F$  and incorporating the horizontal and rotational movements of the soil at the structure's base is:

$$\mathbf{M}\ddot{\mathbf{U}} + \mathbf{C}\dot{\mathbf{U}} + \mathbf{K}\mathbf{U} = \mathbf{F} \quad (10)$$

where  $\mathbf{M}$ ,  $\mathbf{C}$ , and  $\mathbf{K}$  are the mass, damping, and stiffness coefficient matrices respectively;  $\ddot{\mathbf{U}}$ ,  $\dot{\mathbf{U}}$ , and  $\mathbf{U}$  represent the acceleration, velocity, and displacement vectors, respectively and  $\mathbf{F}$  is the impact load vector. Details of the matrices and vectors elements can be defined as:

$$\mathbf{M} = \begin{pmatrix} m_1 & m_1 & m_1 h_1 \\ m_1 & m_1 + m_b & m_1 h_1 \\ m_1 h_1 & m_1 h_1 & m_1 h_1^2 \end{pmatrix}, \quad \mathbf{C} = \begin{pmatrix} c_1 & 0 & 0 \\ 0 & c_h & 0 \\ 0 & 0 & c_r \end{pmatrix}, \quad \mathbf{K} = \begin{pmatrix} k_1 & 0 & 0 \\ 0 & k_h & 0 \\ 0 & 0 & k_r \end{pmatrix}$$

$$\ddot{\mathbf{U}} = \begin{pmatrix} \ddot{u}_1 \\ \ddot{u}_o \\ \ddot{\phi} \end{pmatrix}, \quad \dot{\mathbf{U}} = \begin{pmatrix} \dot{u}_1 \\ \dot{u}_o \\ \dot{\phi} \end{pmatrix}, \quad \mathbf{U} = \begin{pmatrix} u_1 \\ u_o \\ \phi \end{pmatrix}, \quad \mathbf{F} = \begin{pmatrix} F \\ 0 \\ 0 \end{pmatrix}$$

where  $u_1$  is the displacement of the superstructure, while,  $u_o$  and  $\phi$  describe the soil horizontal translation and rocking movements. The corresponding velocities and accelerations are represented with dots i.e., derivatives with respect to time. The dynamic solution to the set of second order ordinary differential equations in Eq. (10) is performed using the finite element toolbox named CALFEM which is the abbreviation of Computer Aided Learning of the Finite Element Method. CALFEM toolbox is available at

[http://www.solid.lth.se/fileadmin/hallfasthetslara/utbildning/kurser/FHL064\\_FEM/calfem34.pdf](http://www.solid.lth.se/fileadmin/hallfasthetslara/utbildning/kurser/FHL064_FEM/calfem34.pdf)

## 6. Response analysis

In this section, numerical illustrations of the formulation developed in this paper for the building model shown in Fig. 3 under blast loads presented in Fig. 2 are provided. In the numerical analysis, the blast pressures have been selected with peaks  $P_{s0}$  of 44.95 kPa, 69.14 kPa, 149.8 kPa, 206.3 kPa and 312 kPa at different stand-off distances  $R$  as well as different positive phase durations  $t_0$ . The system parameters in terms of mass,  $m_1$ , base mass,  $m_b$ , and damping ratio,  $\xi_1$  are set to be  $25 \times 10^3$  kg,  $75 \times 10^3$  kg, 0.05 respectively. The system natural period  $T_n$  is of 1.2 s and the yield strength is taken as  $f_y = 1.369 \times 10^5$  N. The storey height is  $h = 3.5$  m. The parameters of the damage indices are taken as  $\mu_u = 6.0$ , and  $\gamma = 0.15$  (see equations 5, 6 and 7). In the analysis, different soil types classified as very dense, stiff and soft soils have been used (see Uniform Building Code Volume 2 1997). The chosen soil types are characterized with shear wave



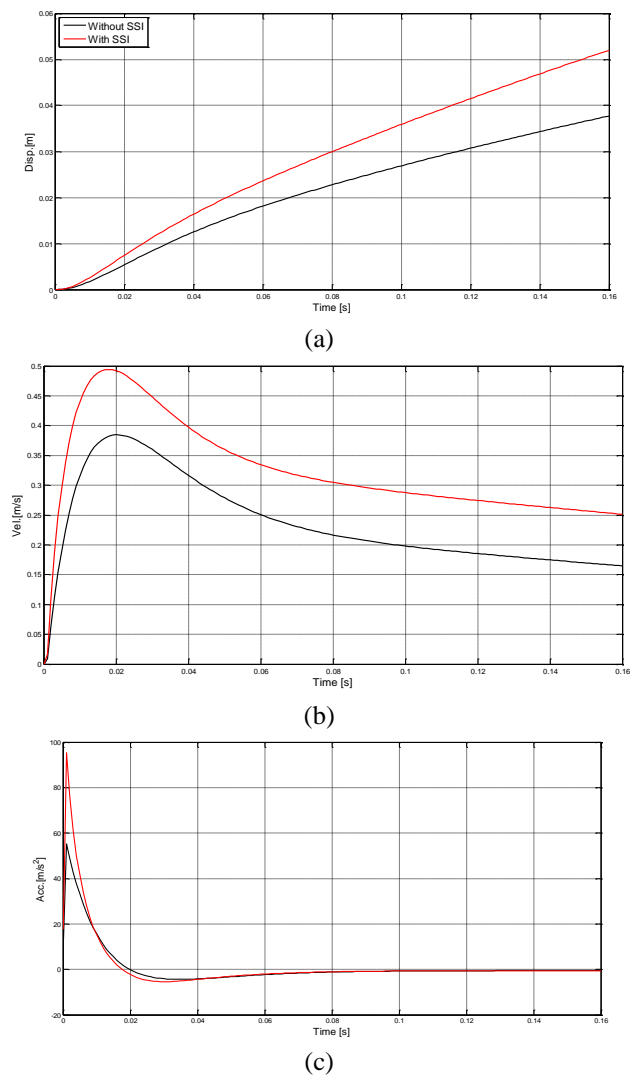


Fig. 5 Storey displacement, velocity and acceleration time histories with and without SSI under blast load

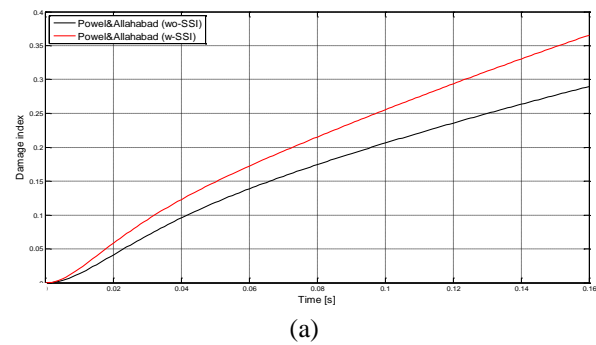


Fig. 6 Continued

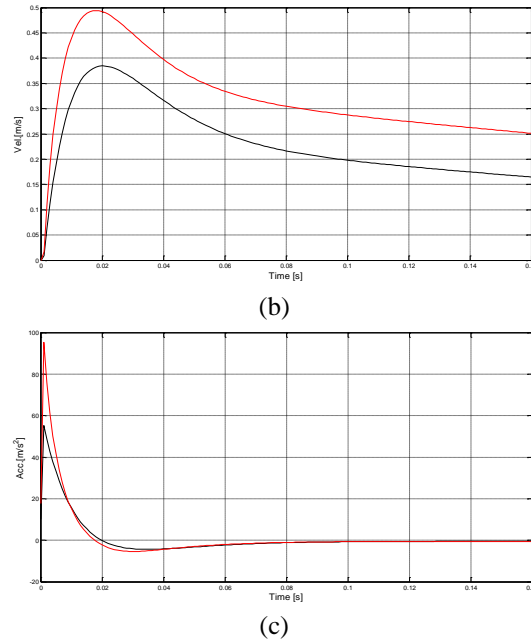


Fig. 6 Powell & Allahabadi, Fajfar & Cosenza and Park & Ang Damage indices time histories with and without SSI under blast load

velocities  $V_s$  of 500 m/sec, 270 m/sec, and 150 m/sec respectively.  $1.8 \times 10^3 \text{ kg/m}^3$ ,  $2.0 \times 10^3 \text{ kg/m}^3$ , and  $2.2 \times 10^3 \text{ kg/m}^3$  respectively denote the chosen soil densities. The radii of equivalent circular foundation for swaying and rocking have been estimated as equal to:  $r_h = r_r = 4 \text{ m}$  (Takewaki 2005). In the time history analysis and for the purpose of investigating the influence of SSI on the building response, the shear wave velocity is taken as 270 m/sec which is changed later to include all the considered herein shear velocities to examine the effect of their variations on the building response and damage as well. The structural response of the building model is calculated Newmark- $\beta$  method in the Matlab platform ( $\alpha = 0.25$ ,  $\beta = 0.50$  and  $\Delta t = 0.005 \text{ s}$ ). The numerical results for the time-history analysis for the building model have been performed under peak blast load  $P_{s0} = 312 \text{ kPa}$  and positive phase durations  $t_0 = 0.02142 \text{ seconds}$  and presented in Figs. 5 and 6. Figs. 7 and 8 present the peak responses and peak damage indices  $DI_{AP}$ ,  $DI_{CF}$  and  $DI_{PA}$  with the variations in building natural period under  $P_{s0} = 312 \text{ kPa}$  and  $69.14 \text{ kPa}$  respectively.

Fig. 5 shows the results for the displacement, velocity and acceleration time-histories of the building model shown in Fig. 3 under blast load without the inclusion of soil flexibility effect and the corresponding results obtained by considering the horizontal and rotational movements of the supporting soil. As shown in the figure, for with and without SSI incorporation, and under blast load, the displacement of the building model reaches its peak at the end of explosion time. The velocity of the superstructure increases rapidly in the initial time as the time increases up to a certain maximum level and decreases as the time increase and then gradually become stable

following the propagation law of blast wave in structures. It is worth noting that the building model reaches its peak velocity almost at time  $t = t_0$ . Focussing on the acceleration curves in Fig. 5 (c), it can be seen that the accelerations reach the peak values immediately after the blast detonation up to a certain maximum value followed by a sudden decrease zero for the remaining time duration. Moreover, it has been noticed that, for with and without SSI inclusion, the acceleration response curves follow almost the same trend as the applied blast load curve. This fact is due to the relatively high impact on structures in short duration of blast wave. Regarding the base soil flexibility effect, it has been noticed that such inclusion significantly increases the obtained displacement and velocity responses during the whole period of the applied blast load. For acceleration response, the influence of the supporting soil flexibility appears to be only significant at the start of the explosion causing sudden increase in the storey accelerations. This sudden increase may lead to damage of equipments and machineries. Moreover, the induced force in the structure due to the explosion and considering SSI effect will be of higher value since this exerted force is proportional to the developed floor acceleration. It has also been noticed that the acceleration response with SSI is nearly identical to the one obtained without SSI effect for the remaining duration time of the explosion and for all the considered blast loads. The captured peak displacement, velocity and acceleration for case ignoring the SSI effect are 0.0379 m, 0.3849 m/s, and 55.1860 m/s<sup>2</sup> respectively. Considering soil flexibility increases these captured values to be 0.0476 m, 0.4989 m/s, and 95.9143 m/s<sup>2</sup> respectively. Consequently, ignoring SSI underestimates the peak responses by 25%, 30% and 74% respectively.

The influence of SSI effects on the damage of the building model under blast load has been evaluated by comparing the predictions obtained by: (i) modelling the building model as fixed at base, (ii) modelling the foundations with equivalent springs to account for the rotational and horizontal movements. Fig. 6 shows that the result from the damage index given by Powell and Allahabad in equation (5) asymptotes close to that obtained using Fajfar and Cosenza in equation (6). Turning now to the results obtained by applying Park and Ang model for measuring damage show a significant difference compared with the two aforementioned models where higher values can be seen in Fig. 6(c). A possible explanation for this might be that Park and Ang model accounts for both maximum plastic displacement and hysteretic energy dissipated to define the structural damage. However, the other two models incorporate either the dynamic response or the dissipated energy for measuring damage. As can be seen in Fig. 6, both damage models confirms that the rotational and horizontal movements of the base soil increase the damaged indices compared with the fixed base building case subjected to blast loads. For the case considering the SSI effect, the damage indices predicted by Powel and Allahabad, Fajfar and Cosenza and Park and Ang were  $DI_{AP} = 0.3655$   $DI_{FC} = 0.2544$  and  $DI_{PA} = 0.6112$  differing from the corresponding values obtained without the inclusion of the base soil flexibility which has been recorded to be  $DI_{AP} = 0.2897$ ,  $DI_{FC} = 0.1786$  and  $DI_{PA} = 0.4562$  respectively. The aforementioned values indicate that the action supporting soil flexibility has great influence on the damage index time-history curves. According to Fajfar and Cosenza recorded damage index and under the considered explosive load, considering soil flexibility changed the building state from insignificant damage to the state of repairable building. Further, Park and Ang also changed the state of building from repairable damage into irreparable for without and with soil flexibility consideration respectively. This confirms the necessity of considering the base soil flexibility in order to predict accurate building damage state under blast effect.

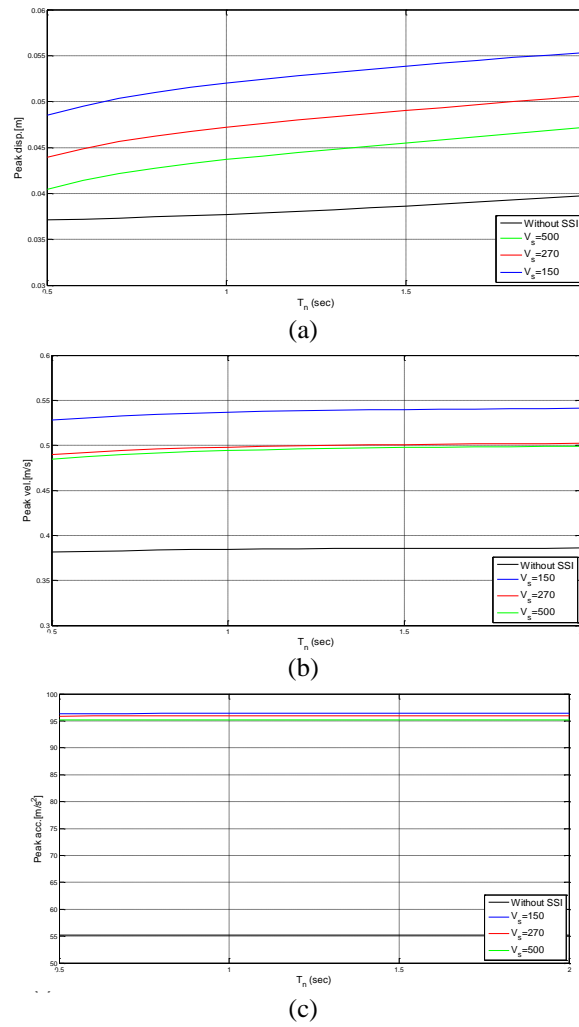


Fig. 7 Variation of peak displacement, velocity and acceleration responses with different natural periods and shear wave velocities

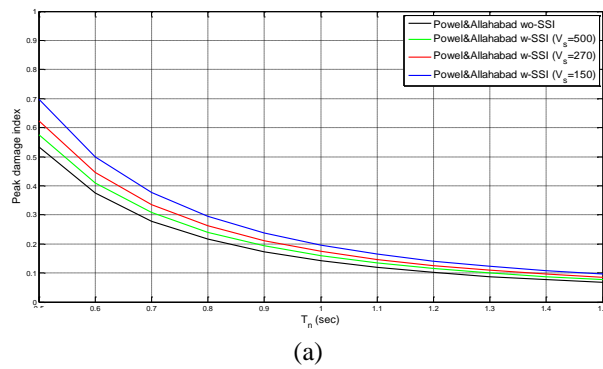
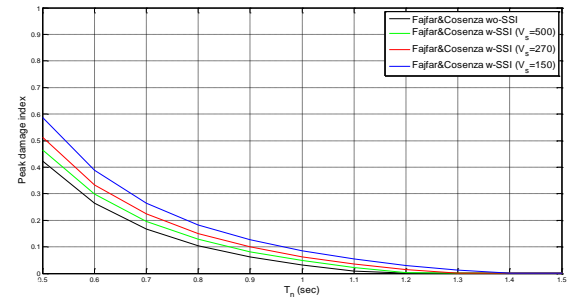
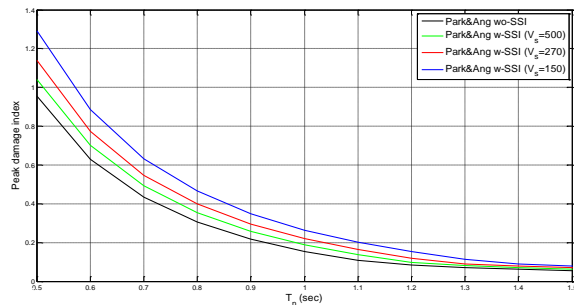


Fig. 8 Continued

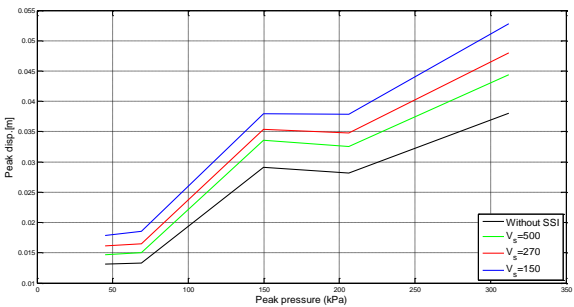


(b)

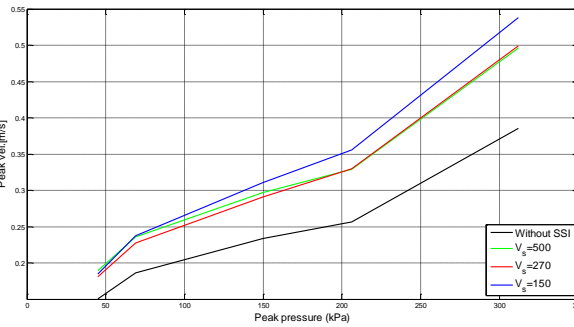


(c)

Fig. 8 Variation of peak Powell and Allahabadi, Fajfar and Cosenza and Park and Ang Damage indices with different natural periods and shear wave velocities

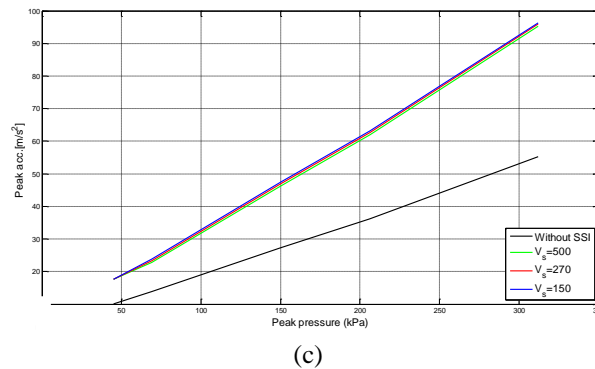


(a)



(b)

Fig. 9 Continued



(c)  
Fig. 9 Variation of peak displacement, velocity and acceleration responses with different peak pressures and shear wave velocities

The variation of the peak displacements, velocities, and accelerations against the natural period  $T_n$  of the building model for different values of shear velocities of the supporting soil are shown in Fig. 7. From the figure, the increase of natural period increases the peak floor displacement; the reason behind this could be explained based on the fact that the increase in natural period increases the building flexibility. The peak velocity is influenced little by the natural period where the increase in periods will transmit slight increase in peak velocity till certain amount of building natural period and with further increase in natural periods the peak velocity remains constant for all the considered shear velocities. The absolute peak acceleration of the superstructure remains nearly unchanged with increasing the natural period. The obtained peak displacements, velocities and accelerations due to the inclusion of SSI are of larger values compared to the corresponding peak values without such inclusion. Although the induced peak accelerations incorporating soil flexibility effect are significantly larger than the induced values ignoring soil flexibility, it has been noticed that the variation in shear velocities of the supporting base soil have a slight influence on the obtained floor peak accelerations. However, such variation in shear velocities significantly affects the induced peak displacements and velocities.

The plots in Fig. 8 (a, b and c), respectively, show the natural period variation of the peak damage indices of Powell and Allahabad, Fajfar and Cosenza and Park and Ang for different values of the supporting base soil shear velocities. As can be seen, the top line shows the peak damage index of soil class with shear wave velocity of 150 m/s whereas the bottom line shows the peak damage index of base considered as rigid. Peak damage indices of soil class with shear velocity of 270 m/s and 500 m/s are between these lines. It can be seen from this figure that, damage indices inversely proportional to the shear wave velocities. The general trend of the peak damage index curves with SSI is similar to the trend of the peak damage index curve assuming fixed base except for the higher values due to the inclusion of soil flexibility effect. It is observed that the peak damage indices are substantially decreasing with the increase in the building natural periods. Consequently, in this case, the possibility of damage due to blast load is reduced when the lateral period increases. However there is always an upper limit, since excessive natural period may lead to increase in the deflections of the superstructure. It once more indicates that the peak curves are sensitive to the shear velocity variations. It is remarkable that the large damage indices are for the lower shear velocities and consequently it can be concluded from the figure that the

lower the shear wave velocity the higher the induced peak damage index. It is apparent from the figure that discrepancies among the curves are significant at low building's natural period.

Fig. 9 shows the peak story displacements, velocities and accelerations against the peak pressure  $P_{so}$  varying in the range of 44.59 to 312 kPa. As expected, the rate of peak displacements, velocities and accelerations increase with the increase of the peak pressures for with and without SSI consideration and for all the considered shear wave velocities. The plots demonstrate that ignoring base soil flexibility underestimates the induced storey peak responses. Note that absolute peak floor accelerations are nearly insensitive to shear velocity variations of the base soil. The sensitivity to the variation of shear velocities is more pronounced in the obtained peak floor displacements and velocities. As noted earlier, the higher the shear velocities, the lower the induced Peak responses. According to the plots shown in Fig. 9, comparing the results of the obtained peak responses incorporating the translation and rotational movements of supporting soil with the corresponding results ignoring such rotation and translation of the base soil show divergence with the increase in explosion peak pressure (i.e., the response with SSI does not approach that of without SSI).

The peak values of the damage indices quantities under different blast loads are presented in Fig. 10. For comparison purpose, the peak values obtained for with and without SSI are plotted in the same graphs. Similar trends have been observed for all damage indices considered including and excluding soil flexibility effect. The trend of the results indicates that, the higher the peak pressure the higher the induced peak damage indices for the both considering and ignoring the effect of base soil flexibility and for all the considered shear wave velocities. It can be observed from the figure that the damage indices of the building model under all the considered blast loads have been influenced by the consideration of SSI. Further, it is to be noted that the Peak damage index quantities are much affected by the SSI consideration at low shear wave velocities showing large discrepancies between the peak damage index results with and without SSI models specifically at high peak pressures.

## 6. Conclusions

A comprehensive investigation on the assessment of dynamic response and the associated damage to a building model rested on rigid and flexible base and subjected to blast loads of different equivalent weights of TNT and detonated at different distances has been conducted. Influence of SSI on the response and damage has been investigated considering three shear wave velocities. The soil flexibility is idealized using nonlinear springs and viscous dashpots placed in parallel. Rigorous analysis has been carried out through a parametric study. Damage evaluation in terms of damage indices was carried out based on the maximum dynamic response and the structure hysteretic energy. The trend of results of this investigation shows that damage and response of superstructure subjected to blast loads varies according to whether the base soil is rigid or flexible, with flexible base soil superstructure sustaining higher responses and damages indices compared to the lower values at rigid base soil subject to the same blast load. This finding is much more pronounced at low shear velocities, i.e. soft soil condition where the building's response and damage may be underestimated if SSI is ignored. Moreover, the analysis of the results indicates that the building's peak acceleration has been found to be insensitive to the variation in natural period and it was not much affected irrespective of the soil types as well. Similar trend has also

been observed for the peak velocity except at low shear velocity. The peak displacement response of the building model also increases as the natural period is extended. Further the inclusion of SSI increases the superstructure peak displacement which is inversely proportional to the shear velocity variations and may increase the probability of a certain damage level to occur at fixed load intensity. Analysing the structure assuming rigid base soil model does not lead to accurate prediction of the response, and hence flexible base soil modelling is essential to reflect dynamic behaviour of the structures under blast loads properly. This allows a more accurate prediction of structural behavior considering calculated local damages. Therefore, the structural capacities are ascertained more realistically and can help in design and/or retrofitting of buildings.

## References

- Baker, W.E., Cox, P.A., Westine, P.S., Kulesz, J.J. and Strehlow, R.A. (1983), *Explosion Hazards and Evaluation*, Elsevier, Amsterdam, 1983.
- Baker, W.E., Cox, P.A., Westine, P.S., Kulesz, J.J. and Strehlow, R.A. (1983), "An Explosion Hazard and Evaluation: Fundamental Studies in Engineering", *Elsevier Scientific Publishing Company, NY*.
- Boutros, M.K. (2000), "Elastic-plastic model of pinned beams subjected to impulsive loading", *J. Eng. Mech.*, **126**(9), 920-927.
- Cosenza, E., Manfredi, G. and Ramasco, R. (1993), "The use of damage functionals in earthquake resistant design: a comparison among different procedures", *Struct. Dyn. Earthq. Eng.*, **22**, 855-868.
- Cosenza, C., Manfredi, G. and Ramasco, R. (1993), "The use of damage functionals in earthquake engineering: a comparison between different methods", *Earthq. Eng. Struct. Dyn.*, **22**(10), 855-868.
- Elliot, C.L., Mays, G.C. and Smith, P.D. (1992), "The protection of buildings against terrorism and disorder", *Proceedings of Institution of Civil Engineers: Structures & Buildings*, **94**(3), 287-297.
- Fardis M. (1995), "Damage measures and failure criteria for reinforced concrete members", *In: Proceedings 10th European Conference on Earthquake Engineering*, Vienna. Rotterdam: Balkema, 1377-1382.
- Forbes, D.F. (1999), "Blast loading on petrochemical buildings", *J. Energy Eng., ASCE*, **125** (3), 94-102.
- Huang, X., Li, J.C and Ma, G.W. (2011), "Soil-Structure Interaction and Pulse Shape Effect on Structural Element Damage to Blast Load", *J. Perform. Construct. Facil.*, **25**, 400-410.
- Houlston, R. and Des Rochers, C.G. (1987), "Nonlinear structural response of ship panels subjected to air blast loading", *Comput. Struct.*, **26**(1/2), 1-15.
- Harris, C.M. and Piersol, A.G. (2002), *Piersol, In: Harris' Shock and Vibration Handbook*, Edited by Harris, C.M. and A.G. Piersol, McGraw-Hill publishing, New York.
- Jacinto, A.C., Ambrosini, R.D. and Danesi, R.F. (2001), "Experimental and computational analysis of plates under air blast loading", *Int. J. Impact Eng.*, **25**: 927-47.
- Jayasinghe, L.B, Thambiratnam, D.P, Perera, N. and Jayasooriya, J.H.A.R. (2013), "Computer simulation of underground blast response of pile in saturated soil", *Eng. Struct.*, **120**(15), 86-95.
- Krauthammer, T., Shahriar, S. and Shanaa, H.M. (1990), "Response of reinforced concrete elements to severe impulsive loads", *J. Struct. Eng.*, **116** (4), 1061-1079.
- Kumar, M., Matsagar, V.A. and Rao, K.S. (2010), "Blast loading on semi-buried structures with soil-structure interaction", *Proceedings of the IMPLAST Conference: October 12-14 Providence, Rhode Island USA*
- Kinny, G.F. and Graham, K.J. (1985), *Explosive Shocks in Air*, New York, Springer- Verlag, Inc.
- Kappos, A.J. (1997), "Seismic damage index for RC buildings: evaluation of concepts and procedures", *Progress in Struct. Eng. Mater.*, **1**(1), 78-87.
- Liu, H. (2009), "Soil-Structure Interaction and Failure of Cast-Iron Subway Tunnels Subjected to Medium Internal Blast Loading", *J. Perform. Constr. Facil.*, **26**(5), 691-701.



- Luccioni, B.M., Ambrosini, R.D. and Danesi, R.F. (2004), "Analysis of building collapse under blast loads", *Eng. Struct.*, **26**, 63-71.
- Ma, G.W., Huang, X. and Li, J.C. (2008), "Damage assessment for buried structures against internal blast load", *Transact. Tianjin Univ.*, **14**(5), 353-357.
- Ma, G.W., Huang, X. and Li, J.C. (2010), "Simplified damage assessment method for buried structures against external blast load", *J. Struct. Eng.*, **136**(5), 603-612.
- McCabe, S.L. and Hall, W.J. (1989), "Assessment of seismic structural damage", *J. Struct. Eng. (ASCE)*, **115**(9), 2166-2183.
- Osteraas, J.D. (2006), "Murrah. building bombing revisited: a qualitative assessment of blast damage and collapse patterns", *J. Perform. Construct. Facil.*, **20**(4), 330-335.
- Park, Y.J., Ang, A.H.S. and Wen, Y.K. (1987), "Damage-limiting aseismic design of buildings", *Earthq. Spect.*, **3**(1), 1-26.
- Park, Y.J. and Ang, A.H.S. (1985), "Mechanistic seismic damage model for reinforced concrete", *J. Struct. Eng., ASCE*, **111**(4), 722-739.
- Park, Y.J., Ang, A.H.S. and Wen, Y.K. (1985), "Seismic damage analysis of reinforced concrete buildings", *J. Struct. Eng., ASCE*, **111**(4), 740-757.
- Powell, G.H. and Allahabadi, R. (1988), "Seismic damage prediction by deterministic methods: concepts and procedures", *Earthq. Eng. Struct. Dyn.*, **16**, 719-734.
- Powell, G.H. and Allahabadi, R. (1988), "Seismic damage predictions by deterministic methods: concepts and procedures", *Earthq. Eng. Struct. Dyn.*, **16**(5), 719-734.
- Rudrapatna, N.S., Vaziri, R. and Olson, M.D. (1999), "Deformation and failure of blast-loaded square plates", *Int. J. Impact Eng.*, **22**, 449-467.
- Schleyer, G.K. and Hsu, S.S. (2000), "A modelling scheme for predicting the response of elastic-plastic structures to pulse pressure loading", *Int. J. Impact Eng.*, **24**(8), 759-777.
- Shi, Y.C., Hao, H. and Li, Z.X. (2007), "Numerical simulation of blast wave interaction with structure columns", *Int. J. Shock Waves*, **17**, 113-133.
- Smith, P.D. and Hetherington, J.G. (1994), *Blast and Ballistic Loading of Structures*, Butterworth-Heinemann Ltd., Linacre House, Jordan Hill, Oxford.
- Tang, E.K.C. and Hao, H. (2010), "Numerical simulation of a cable-stayed bridge response to blast loads, Part I: Model development and response calculations", *Eng. Struct.*, **32**, 3180-3192.
- Tang, E.K.C. and Hao, H. (2010), "Numerical simulation of a cable-stayed bridge response to blast loads, Part II: Damage prediction and FRP strengthening", *Eng. Struct.*, **32**: 3193-3205.
- Takewaki, I. (2005), "Bound of earthquake input energy to soil-structure interaction systems", *Soil Dyn. Earthq. Eng.*, **25**, 741-752.
- Williams, M.S. and Sexsmith, R.G. (1995), "Seismic damage indices for concrete structures: a state of the art review", *Earthq. Spect.*, **11**(2), 319-349.
- Whitman, R.V. and Richart, F.E. (1967), "Design procedures for dynamically loaded foundations", *J. Soil Mech. Found. Div. ASCE*, 93(SM6).